Heating and de-icing function in conductive concrete and cement paste with the hybrid addition of carbon nanotubes and graphite products

OPEN ACCESS
IOP Publishing
Smart Materials and Structures
Smart Mater. Struct. **30** (2021) 045010 (12pp)
https://doi.org/10.1088/1361-665X/abe032

Heating and de-icing function in conductive concrete and cement paste with the hybrid addition of carbon nanotubes and graphite products

C Farcas, O Galao, R Navarro, E Zornoza, F J Baeza, B Del Moral, R Pla and P Garcés

Civil Engineering Department, University of Alicante, Ctra. San Vicente s/n, 03690 San Vicente del Raspeig, Spain

E-mail: pedro.garces@ua.es

Received 30 October 2020, revised 8 January 2021
Accepted for publication 26 January 2021
Published 26 February 2021

Abstract

This paper aims to study the viability of conductive cement paste and conductive concrete with the hybrid addition of carbon nanotubes (CNT) and graphite powder (GP) as a self-heating material for heating, ice formation prevention and de-icing in pavements. Different heating tests, ice-preventing tests and de-icing tests were performed with cement paste and concrete specimens. Results confirm that the conductive cement composites studied, with the addition of 1% CNT + 5% GP, exhibited heating, de-icing and ice-prevention properties, when applying constant AC/DC voltages between the two end sides of each specimen, with relatively low energy consumption. The main contribution of this work is to achieve a sufficient conductivity level for the development of the heating and de-icing function using this hybrid addition in concrete, which has not been used so far, in order to be applied in real concrete structures.

Keywords: cement composites, multi-walled carbon nanotubes, graphite, heating, de-icing

(Some figures may appear in colour only in the online journal)

1. Introduction

In the recent years, the addition of carbon-based materials to cement composites has promoted a disruption in the functions that can be performed by the traditional structural materials in the construction and building field. Typically, the carbon additions to which more attention has been paid are carbon fibres (CF), carbon nanofibres (CNF) and carbon nanotubes (CNT). This new area of research has been based in the modification of the electrical conductivity of these carbon-cement composites [1]. The research interest has been focused in developing functions such as: strain sensing [2–5], resistance to corrosion phenomena [6–8] and electromagnetic interference shielding [9].

Nevertheless, one of the most powerful and current functions that a conductive cement-based material can perform is the possibility of heating. Yehia *et al* [10] and Chung [11] pioneered the development of this function using conductive cements based materials. The use of materials that could offer the possibility of increasing their temperature in transport infrastructures such as bridges or airports, would avoid the use of corroding salts that could damage the steel reinforcements.

The self-heating function in carbon-cement composites is observed due to Joule effect, i.e. the typical heating mechanism of an electric resistance which is produced by the

dissipation of the kinetic energy of the moving electrons within an electric field when they interact with atoms of the material. When this concept is applied to structural materials, it is possible to use the structural material itself to provoke the melting of the ice on its surface (or to avoid its formation).

Different conductive additions have been incorporated in cementitious heating composites, such as steel fibre, steel shaving [12], CF [13–16], CNF [17], graphite [18], CNT [19] or even shape memory alloy [20]. Some of these materials, such as steel fibres, show some technical problem. It is observed that conductive cement based materials containing steel fibres present a decrease in the conductivity over time. This yields this material to a worse response from the point of view of the development of the heating function [21]. Other authors have studied the development of this function using different carbonaceous materials addition, such us CF, by Sassani *et al* [15], CNF by Galao *et al* [17], graphite by Qin *et al* [18] or CNT by Kim *et al* [22]. In general, results show the viability of using these materials from the point of view of achieving to prevent ice formation. Nevertheless, Yehia *et al* [23] showed that the combination of CF with CNT implies a better behaviour concerning the heating function due to the contact areas between CF and CNF, that decreases the damage of electrically conductive pathways during heating.

Cement composite's electrical properties can be modified with the addition of graphite powder (GP), which is a well-known carbon product. There are different studies in which graphite is used as a carbonaceous addition to generate conductive cement paste that allows other functions to be carried out, such as electrochemical techniques [6–8] or self-sensing function, as a component of a hybrid addition to CF. On the other hand, as mentioned previously, there are numerous investigations carried out using CNT as the only addition in the development of the self-sensing function in cement-based materials.

This research is focussed on exploring the heating, ice-prevention and de-icing behaviour of conductive concrete with the hybrid addition of both CNT and GP and comparing these results with cement pastes with the same addition. Due to the fact that nano-scale conductive fillers (e.g. CNT) are more expensive than those at the micro-scale ones (e.g. graphite), a conductive cement-based sensor using hybrid fillers has an economic advantage.

This research has been carried out in the framework of the European project MASTRO. According to this project, the main objectives are focused on the development of conductive multifunctional cement-based materials, for specific applications in the area of civil engineering and architecture using hybrid CNT and graphite based materials.

The main contribution of this work is to achieve a sufficient conductivity level for the development of the heating and de-icing function using this hybrid addition in concrete, which has not been tested so far. In conductive cement paste, with the same dosage of carbonaceous additions referred to cement mass, the conductivity level is one order of magnitude higher. This justifies the comparative study carried out between paste and concrete.

Table 1. Main properties of C100 CNT (supplied by Arkema).

Description	CCVD multi-wall carbon nanotubes C100	
Appearance	Black powder	
Powder characteristics	Apparent density	50–150 kg m^{-3}
	Mean agglomerate size	200–500 μm
	Weight loss at 105 °C	<1%
CNT characteristics	C content	>90 wt%
	Free amorphous carbon	Not detectable
	Mean number of walls	(SEM/TEM)
	Outer mean diameter	5–15
	Length	10–15 nm
		0.1–10 μm

Table 2. Graphite powder ABG1010 (supplied by Superior Graphite).

Description	Purified expanded graphite ABG1010	
Appearance	Black powder	
Powder characteristics	True density	2.25 g cm^{-3}
	Surface area BET	22 m^2 g^{-1}
	Loss of ignition (LOI)	99.95%
Particle size	C content	>90 wt%
	Particle size distribution d10	3.3 μm
	Particle size distribution d50	9.8 μm
	Particle size distribution d90	40.2 μm

2. Materials and methodology

2.1. Materials, mix proportions and fabrication

The materials used were Portland cement type CEM I 52.5R, supplied by Cemex Spain S.A., CNT Graphistrenght C100, supplied by Arkema, which main properties are shown in table 1, graphite powder ABG1010, supplied by Superior Graphite, which main properties are shown in table 2, superplasticizer Sika Viscocrete 20-HE, supplied by SIKA, standard silica sand, limestone gravel, silica fume Sika Fume®, supplied by SIKA and distilled water.

The dosages used for both composites are shown in table 3, which had 1% C100 + 5% ABG1010, referred to cement mass, as conductive addition. In order to optimize the CNT dispersion in the mix, the procedure describe in [24] was strictly applied.

Prismatic cement paste specimens of standard size (dimensions 4 cm × 4 cm × 16 cm) were fabricated according to the Spanish Standard UNE-EN 196-3:2017 and concrete specimens of dimensions 4 cm × 15 cm × 15 cm. After 24 h curing in humidity chamber at 20 °C, >95% relative humidity, the specimens were demoulded and kept in >95% relative humidity environment for 28 d.

2.2. Heating test

Heating tests were performed in laboratory conditions, after curing period, (approximately at 23 °C and RH 60%). Tests

Table 3. Dosages of conductive paste and concrete.

	C100[a]	ABG1010[a]	w/c	Cement	Coarse aggregate	Fine aggregate[b]	Silica fume	Water	Plasticizer[a]
Paste	1%	5%	0.4	1800 g	—	—	—	720 g	2%
Concrete	1%	5%	0.6	5400 g	6075 g	4050 g	540 g	3240 g	3%

[a]Referred to cement mass.
[b]Silica sand.

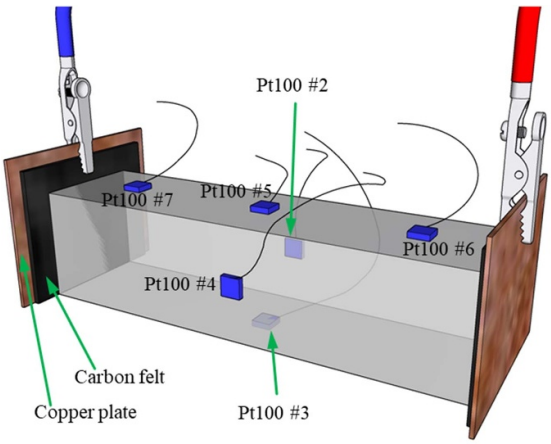

Figure 1. Sketch of a conductive cement paste specimen ready to be tested.

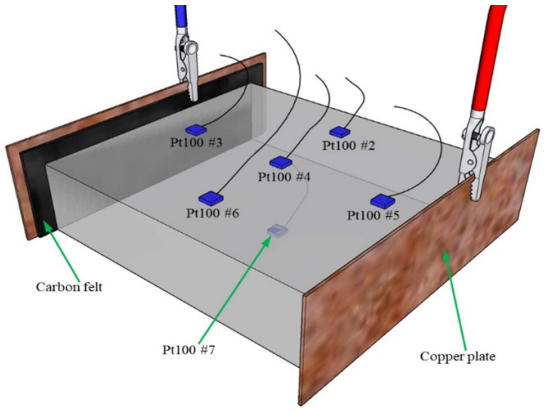

Figure 2. Sketch of a conductive concrete slab ready to be tested.

consisted on applying different constant voltages in alternating current (AC) and direct current (DC) between the two end sides of the conductive specimens (4 × 4 cm^2, paste, and 4 × 15 cm^2, concrete). Opposite sides of the specimens were painted with silver paint. Before testing, a 2 mm thick carbon felt and a 0.5 mm thick copper plate were placed in contact to the silver painted sides and the whole package anchored with a passive bar clamp, for optimal power delivery.

The temperature values on different points of specimen surface were monitored by six resistance temperature detectors type Pt100 connected to a data logger. A thermographic camera was used in order to achieve the temperature distribution. Figures 1 and 2 show a sketch of a cement paste specimen, and a concrete specimen, respectively, ready to be tested. Heating tests consist on applying different voltages for each specimen. The higher the applied voltage, the higher the monitored temperature. Figure 3 shows different images corresponding to different temperatures reached when applying increasing voltages.

Different fixed voltages were applied with a digital direct power source (DC) and an alternating power source F5V (AC, at 50 Hz). In both cases, electrical current was measured with digital multimeters Keithley 2002. As aforementioned, six Pt100 sensors were situated on the surface of each specimen in order to monitor its surface temperature, according to figures 1 and 2, and another two Pt100 sensors were placed to control de environment temperature (room).

At least three different specimens of two mix sets where tested in all cases.

2.3. *Ice-prevention and de-icing tests*

After the heating tests in laboratory conditions, the specimens were exposed to the same fix voltages with AC and DC, for ice-prevention tests and de-icing tests. A Liebherr freezer was utilized with inner dimensions of 1.45 m × 0.50 m × 0.65 m. The freezer average environment temperature was −15 °C.

In ice-prevention tests, specimens were firstly introduced into a freezer, until they reached +5 °C, the power source (AC or DC) was turned on at a fixed voltage. The aim was to apply a fixed voltage enough to keep the specimen's temperature above approximately +3 °C, in order to prevent the formation of ice. After steady temperature was reached, the power source was turned off. The evolution of temperature was continuously registered during each test.

In the de-icing tests, specimens were previously placed in the cooler for a period of 24 h, approximately. As a consequence, the temperature sensors of the samples reached an initial temperature of −15 °C. Then the power source (AC or DC) was connected at a fixed voltage, hence increasing the specimen's temperature accordingly to the supplied power. The aim, in this case, was to apply a fixed voltage enough to increase the specimen's temperature above approximately +3 °C, in order to avoid the presence of a stable ice layer. After about 5 h, the power source was turned off. The temperature and the electrical current were monitored during all tests. At least three different specimens of two mix sets where tested in all cases.

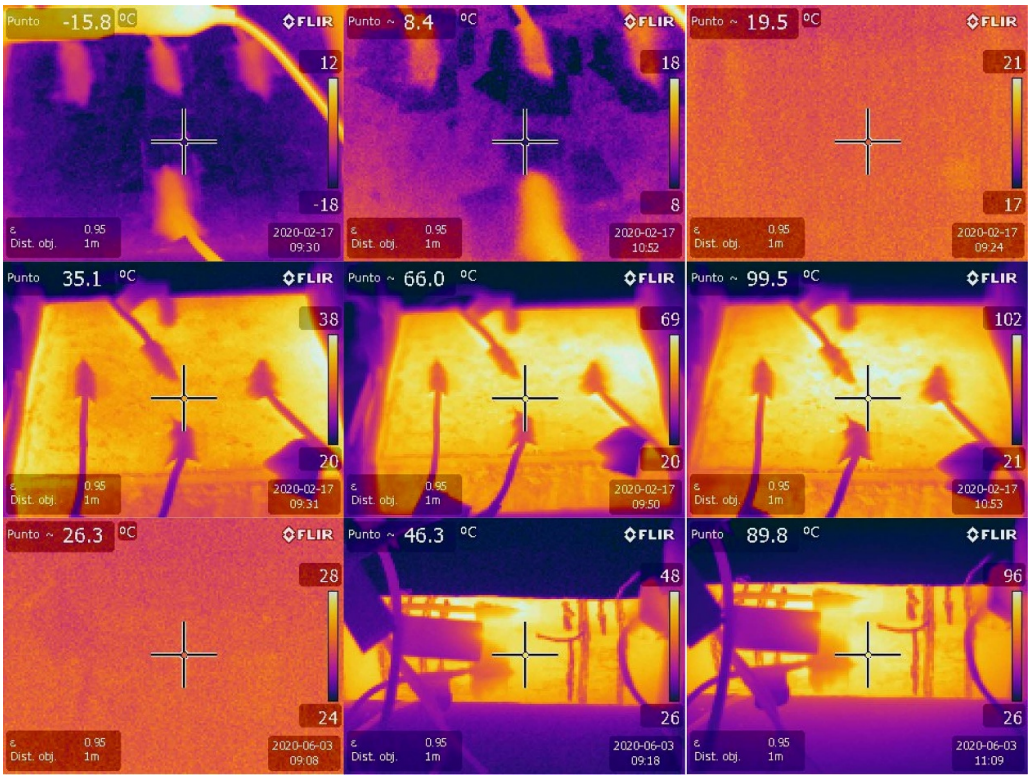

Figure 3. Thermographic pictures of different tests and different specimens.

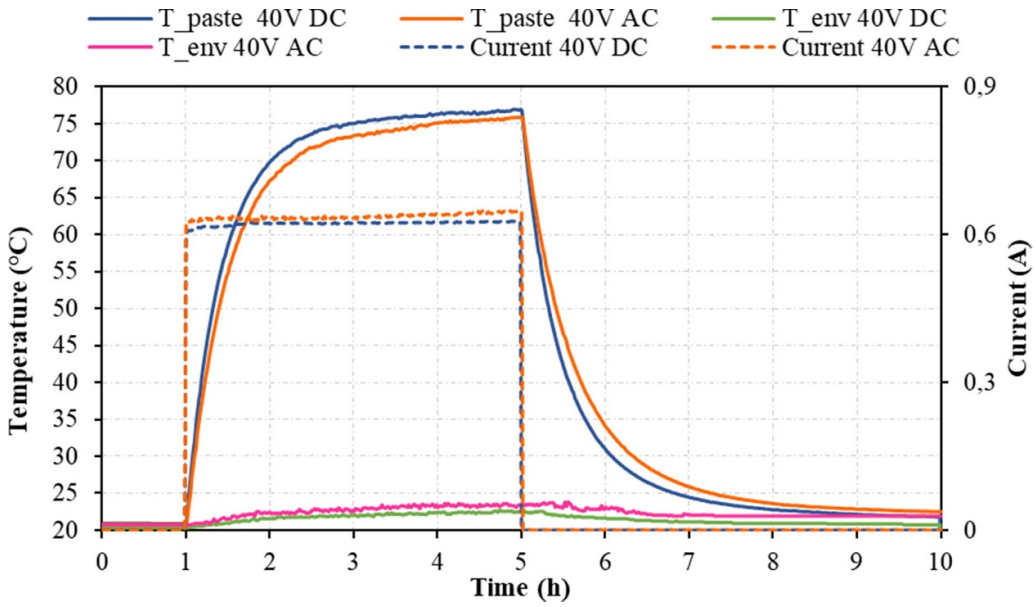

Figure 4. Environment (room) temperature (T_env), specimen's average temperature (T_paste), both in °C, and the monitored current (dashed lines), in A, versus time, in h, for cement paste AC and DC heating tests with 40 V fixed voltage.

3. Results and discussion

3.1. Study of the heating function in conductive cement paste

Different tests with different fixed voltages were performed. As expected, the higher the fixed voltage, the higher the specimen's temperature was obtained. All test types were performed with both AC and DC. In all cases, negligible differences were obtained for the same fixed voltage with both AC and DC power.

Figure 4 shows the results obtained for 1% C100 + 5% ABG1010 cement paste specimens with 40 V AC and DC applied voltage. The specimen's temperature average values for both tests and the monitored current (dashed lines) are

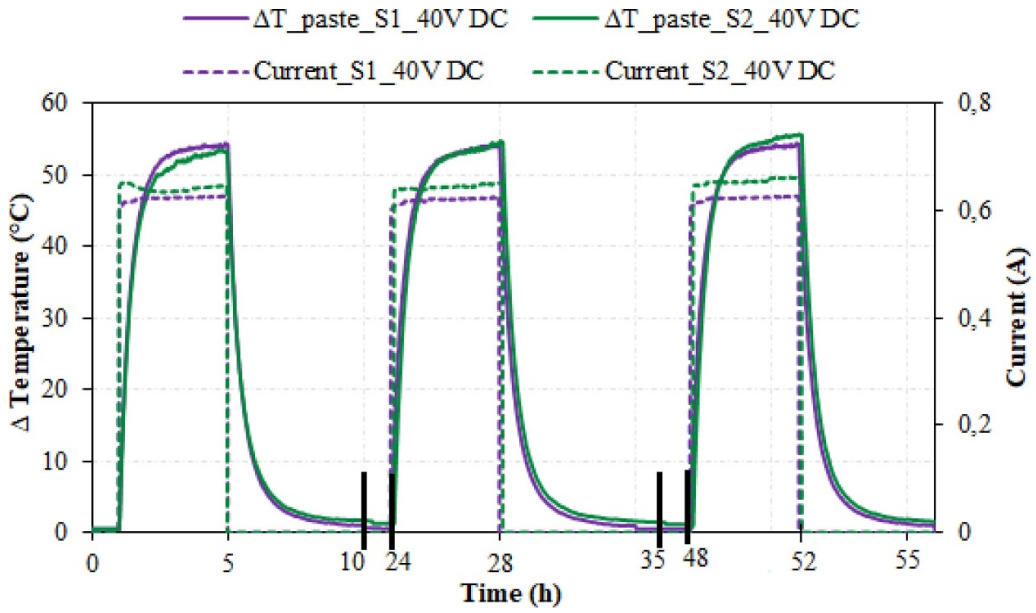

Figure 5. Temperature variation (°C) and monitored electrical current (A), versus time (h), for two cement paste specimens, of three consecutive 40 V DC heating tests.

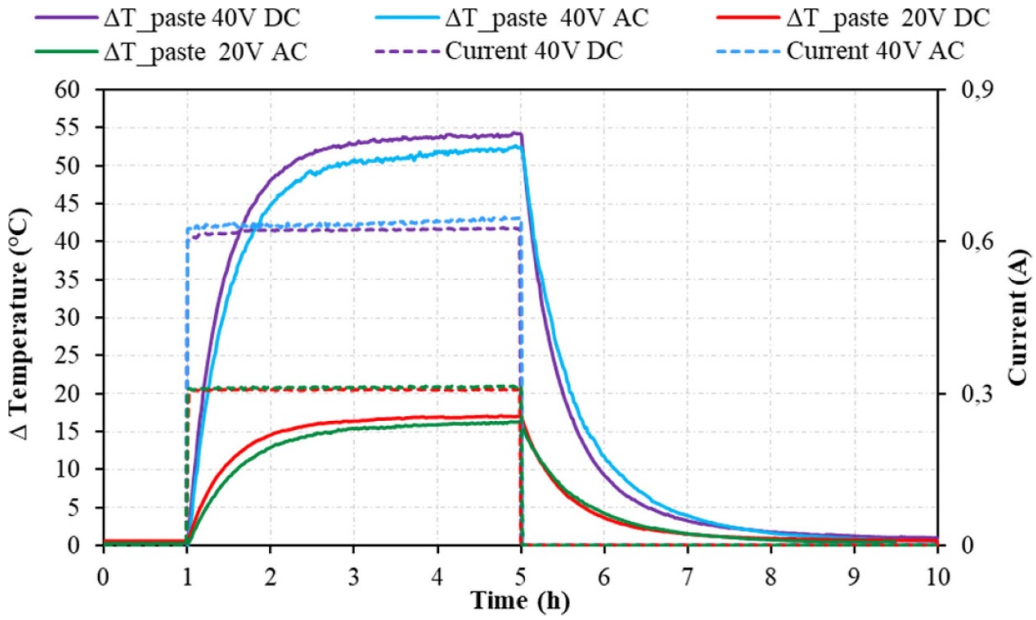

Figure 6. Temperature variation (°C) and monitored electrical current (A), versus time (h), for cement paste AC and DC heating tests with 20 V and 40 V fixed voltages.

depicted. As it can be observed, when the power is turn on the specimen's temperature starting from around 21 °C to 23 °C increases up to a constant value of around 75 °C. As previously indicated, negligible differences in the temperature were monitored when applying DC or AC voltages. In AC tests, an increase of +20 °C was obtained after 15 min and 90% of the maximum temperature reached (+47.5 °C increase) was obtained after 1 h and 14 min, while the electrical current was monitored at a steady level throughout the whole test at 0.64 A. In DC test, an increase of +20 °C was obtained after 13 min and 90% of the maximum temperature reached (+47.9 °C increase) was obtained after 1 h and 11 min, while the electrical current was monitored at a steady level throughout the whole test at 0.62 A. As voltage and current kept constant throughout the tests, the electrical resistance of the specimens remained constant with the temperature variation.

Figure 5 shows the temperature variation, in °C, and the monitored electrical current, in A, versus time, in h, of three consecutive heating tests with two different specimens of two different batches. As it can be observed, the results are quite similar, hence confirming repeatability (same behaviour of one single specimens to different tests) and reproducibility (same behaviour of different specimens to the same test).

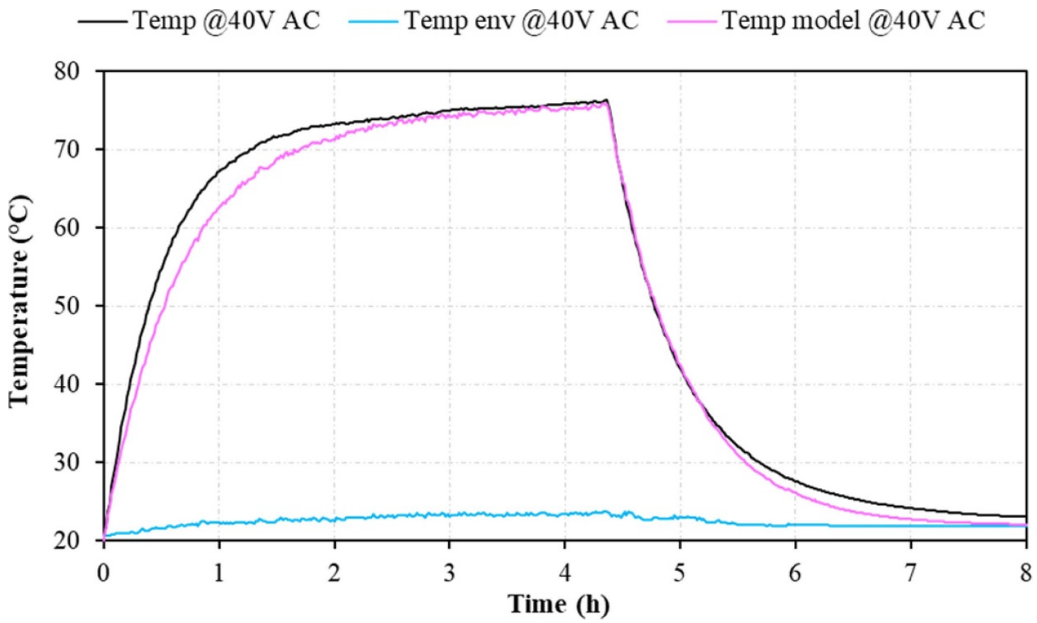

Figure 7. Experimental temperature (black line) and model temperature (violet line), versus time, for a 40 V AC conductive paste specimen heating test. The blue line represents the environment experimental temperature.

Considering cold regions with environment temperatures between −5 °C and −10 °C, increasing the composite's temperature in about +15 °C could be enough to avoid the formation of ice in the pavement. Figure 6 shows the increment of temperature, in °C, and the electrical current, in A, versus time, for heating tests with paste specimens at 20 V and 40 V DC and AC. With 20 V tests, the increment of temperature was +17 °C for both current types (0.308 A DC and 0.312 A AC) which could be enough variation for de-icing systems with environment temperature above −15 °C. The figure also includes the results shown in figure 4, in order to compare the differences. As it can be observed, doubling the fixed applied voltage implies doubling the electrical current, which implies steady resistivity of the composites in the shown temperature range. On the other hand, the maximum reached temperature at 40 V (AC and DC) is around 3.3 times higher than the maximum reached temperature at 20 V (AC and DC).

In order to model the mechanism of heating, a previously reported model was applied [13]. Using the equations and parameters from the aforementioned model, all the experimental tests have been simulated. As an example, figure 7 shows the experimental temperature (black line) and model temperature (violet line), versus time, for a 40 V AC conductive paste specimen heating test. The blue line represents the environment experimental temperature. The fitting level of both curves is significant. So, the optimized conductive cement-based material could be determined with this tool, by analysing the minimum power required to obtain a desired temperature.

3.2. Study of the heating function in conductive concrete

As previously commented, six temperature sensors were attached to each specimen. During the tests, differences in the temperature of the sensors were negligible, which indicates that the temperature distribution throughout the whole surface of the specimens was relatively uniform. Figure 8 shows a conductive concrete heating test with an applied fixed voltage of 65 V AC. The temperature monitored in the eight temperature Pt100 sensors and the monitored current, versus time, are depicted. Sensors Pt100 #1 and Pt100 #8 were used to monitor the environment temperature and the rest were attached to the specimen. It can be observed that Pt100 #7 showed the highest temperature being located at the bottom of the specimen, were heat loss is lower, as the specimen is resting on a refractory brick. Temperature sensors #3, #4 and #5, which are centrally aligned between electrodes, showed approximately the same temperature throughout the whole test, slightly below sensor #7 (2 °C–3 °C), which clearly confirms the temperature distribution uniformity. Sensors #2 and #6 showed lower temperature than the former sensors, which is in accordance with the proximity to the specimen's edge, where temperature loss is higher. The dotted black line in the figure shows the average temperature of Pt100 sensors from #2 to #7, which is almost coincident with sensor #5.

In order to clearer observe the aforementioned temperature uniformity, table 4 shows the temperatures of all Pt100 sensors at the beginning of the test (T_0), after 1 h (T_{1h}), after 4 h (T_{4h}) and the maximum temperature recorded (T_{max}), for the former 65 V fixed voltage AC heating test. Furthermore table 5 depicts the average temperature of Pt100 sensors #2, #3, #4, #5, #6 and #7 after 0 h, after 1 h and 10 min, and after 4 h (T_0, T_{1h} 10 min and T_{4h}, respectively, in °C), and also the central point IR camera temperature registered at the same test times. It can be observed that the differences are negligible. The corresponding IR thermal images are shown in figure 9.

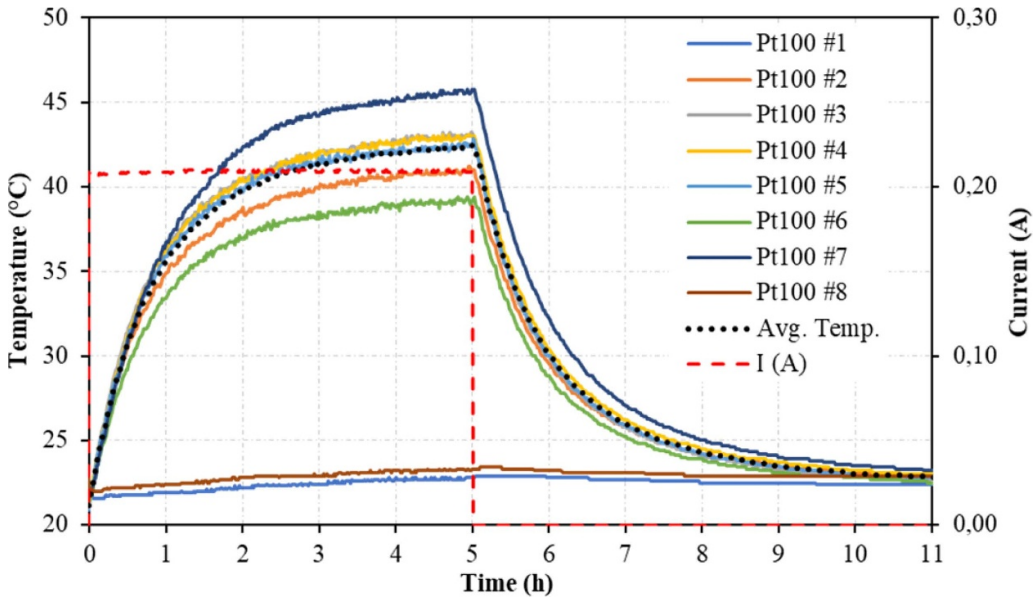

Figure 8. Environment temperature (Pt100 #1 and Pt100 #8), specimen's temperature at different positions (Pt100 #2–Pt100 #7), specimen's average temperature calculated with Pt100 #2–Pt100 #7, in °C, and the monitored current (dashed lines), in A, versus time, in h, for a concrete 65 V fixed voltage AC heating test.

Table 4. Temperatures of all Pt100 sensors at the beginning of the test (T_0), after 1 h (T_{1h}), after 4 h (T_{4h}) and the maximum temperature recorded (T_{max}), for a 65 V fixed voltage AC heating test.

Heating AC test 65 V	PT100 #1[a]	PT100 #2	PT100 #3	PT100 #4	PT100 #5	PT100 #6	PT100 #7	PT100 #8[a]
T_0 (°C)	21.7	21.4	21.2	21.6	21.3	21.3	21.8	22.2
T_{1h} (°C) (after 1 h)	21.9	35.5	37.2	36.9	36.8	34.3	37.8	22.4
T_{4h} (°C) (after 4 h)	22.6	40.5	42.8	42.6	42.2	38.9	45.1	23.2
T_{max} (°C)	22.9	41.2	43.2	43.1	42.9	39.4	45.8	23.4

[a]Room temperature.

Table 5. Average temperature of Pt100 sensors attached to the specimen (#2, #3, #4, #5, #6 and #7) after 0 h, after 1 h and 10 min, and after 4 h (T_0, $T_{1h\ 10min}$ and T_{4h}, respectively, in °C), and the central point infrared (IR) camera temperature registered at the same test times, for a 65 V fixed voltage AC heating test.

Heating AC test 65 V	Average temperature[a]	Central point IR camera temperature
T_0 (°C)	21.4[a]	21.3
$T_{1h\ 10min}$ (°C)	36.7[a]	37.8
T_{4h} (°C)	42.0[a]	43.6

[a]Average temperature of Pt100 sensors #2, #3, #4, #5, #6 and #7.

Table 6. Heating rate in °C min^{-1}, and the time in minutes necessary to increase the temperature +20 °C, for 65 V, 90 V and 150 V DC heating tests.

Voltage (V)	Heating rate (°C min^{-1})	Time to increase +20 °C (min)
65 V DC	0.27	73.3
90 V DC	0.54	37.4
150 V DC	1.54	13.0

As in the previous conductive cement paste tests, the calculated average temperature value will be shown in the next figures.

At least three specimens were tested at least three times at each fixed AC and DC voltages. Results were similar for each specimen and repetition. Hence, the values shown in the following figures are exclusive of one single test but represent the whole series.

Figure 10 shows the increment of temperature and the electric current, versus time, for 65 V, 90 V and 150 V fixed DC voltages tests with concrete specimens. A maximum increment of 19 °C was obtained at 65 V, 34 °C at 90 V and 78 °C at 150 V (with maximum reached temperatures of 42 °C at 65 V, 58 °C at 90 V, and 100 °C at 150 V). The average electrical current was 0.208 A for 65 V tests, 0.295 A for 90 V tests, and 0.506 A for 150 V tests. The average power, in W m^{-2}, was 202 at 65 V, 396 at 90 V, and 1134 at 150 V. For both current types (AC and DC) results were similar, with similar increment of temperature, current and power applied. In order

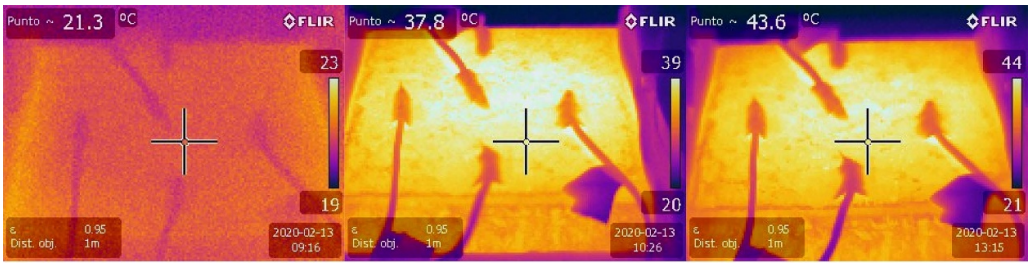

Figure 9. Infrared images related in table 5.

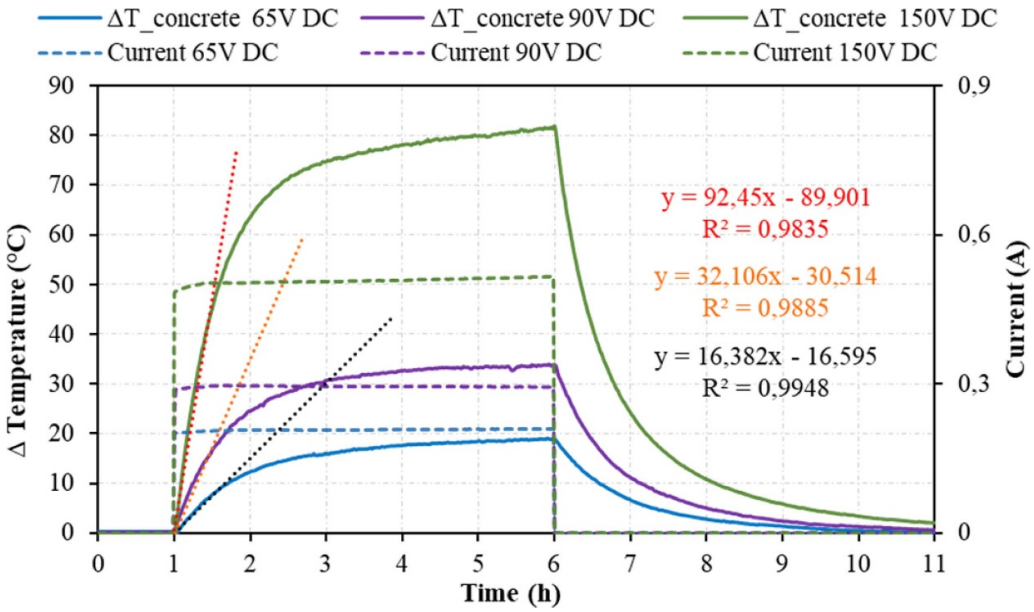

Figure 10. Specimen's average incremental temperature (°C) and electrical current (A), versus time (h), for 65 V, 90 V and 150 V fixed voltage DC tests. The dotted lines represent the linear regression function for the first 0.5 h data (black for 65 V DC heating test, orange for 90 V DC test, and red for 150 V DC test). Equations and coefficients of determination (R^2) are also included in the dotted lines' corresponding colours.

to determine the heating rate, i.e. the velocity of the temperature variation with time in the first 30 min after system connection, a simple regression analysis of each test is also depicted in the figure (black dotted line for 65 V DC test, orange dotted line for 90 V DC test, and red dotted line for 150 V DC test). Equations and coefficients of determination (R^2) are also included in the figure. The coefficient of x represents the slope of the line, i.e. the heating rate, in °C h^{-1}). An increment of +20 °C could be enough for most practical applications. Hence, the obtained heating rates in °C min^{-1}, and the time in minutes necessary to increase the temperature +20 °C are shown in table 6. Results of conductive concrete tests applying 150 V are in accordance with different prior studies with cement pastes: (a) cement pastes with 37 vol% graphite powder, 1.6 °C min^{-1} [25]; (b) cement pastes with 12 vol% nickel particles, 1.5 °C min^{-1} [26]; (c) cement pastes with 1% CNT by cement mass, 1.6 °C min^{-1} [17]. As expected, the heating rate increases with higher voltages and the time to increase +20 °C decreases as the voltage increases. Hence, in accordance with the required needs, the fixed voltage applied could control the time necessary to obtain a determined temperature.

Table 7 summarizes the electrical characteristics (resistivity, current type and fixed voltage applied), temperature variation and energy characteristics (average power, consumed energy and average energy consumption) of heating tests. The calculated test cost in € is also included calculated considering 0.15€ kW^{-1} h^{-1}, being the 2019 approximate Spain commercial electric price.

In all cases, high temperature increments can be obtained with relatively small voltage and electrical current. In fact, the current type seems not to play an important role in the thermal behaviour and the energy performance of the different composites fabricated. The specimen's resistivity remains stable in all conditions for each composite. Concrete specimen's resistivity was 16 times higher than the one for cement paste specimens. Similar temperature increment can be observed for concrete at 65 V and paste at 20 V, but with higher average power and average energy consumption in the case of paste specimens, although, on the other hand, the consumed energy and the cost was higher in the case of concrete specimens. The cost per unit of area to increase 19 °C the temperature of the studied concrete, for 5 h, with the specified configuration (65 V) was 0.152€ m^{-2}, for both AC and DC.

Table 7. Summary of the electrical characteristics (resistivity, current type and fixed voltage applied), temperature variation and energy characteristics (average power, consumed energy and average energy consumption) of heating tests. The calculated test cost in € is also included.

	Heating								
Type	Resistivity (Ω cm)	AC/DC	Voltage (V)	Current (A)	ΔT (°C)	Average power (W m^{-2})	Consumed energy (kW h)	Cost (€)	Average energy consumption (kW h m^{-2})
Concrete	1049	DC	65	0.208	18.8	202	0.067	0.0101	1.01
	1044	AC	65	0.209	19	203	0.068	0.0102	1.02
	1026	DC	90	0.295	33.8	396	0.132	0.0198	1.97
	1047	AC	90	0.289	34.5	388	0.130	0.0195	1.94
	996	DC	150	0.506	79.5	1134	0.378	0.0567	5.65
	1039	AC	150	0.485	76.5	1087	0.376	0.0564	5.62
Paste	67	DC	20	0.310	17.1	304	0.025	0.0037	1.21
	64	AC	20	0.312	17	325	0.028	0.0043	1.40
	58	DC	40	0.622	53.2	1228	0.099	0.0149	4.89
	63	AC	40	0.638	52.8	1329	0.111	0.0167	5.50

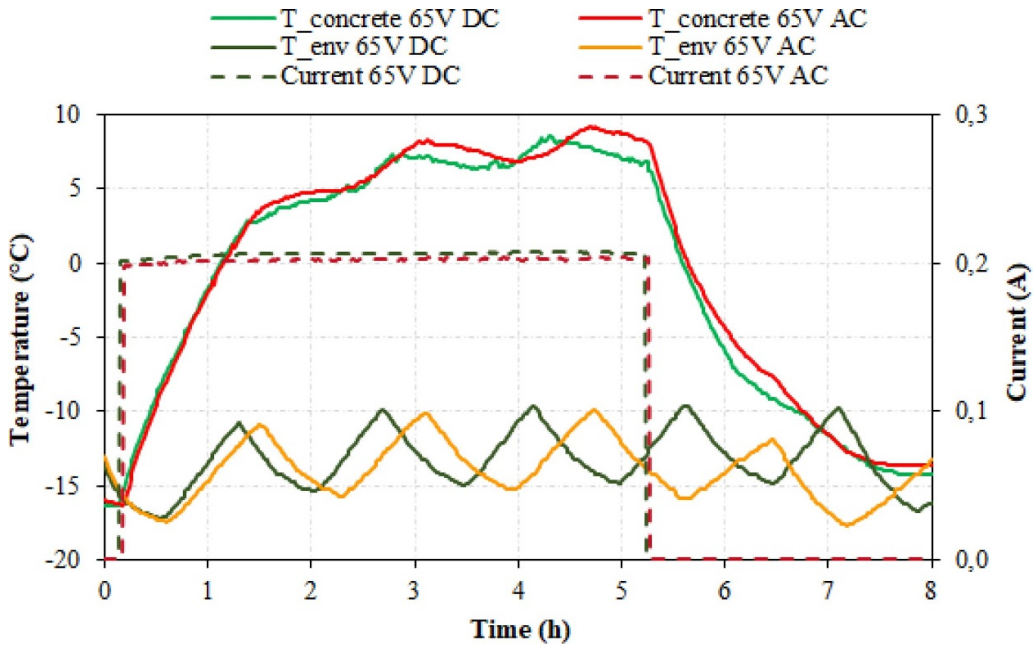

Figure 11. Environment (freezer) temperature (T_env), specimen's average temperature (T_concrete), both in °C, and the monitored current (dashed lines), in A, versus time, in h, for concrete 65 V fixed voltage AC and DC de-icing tests.

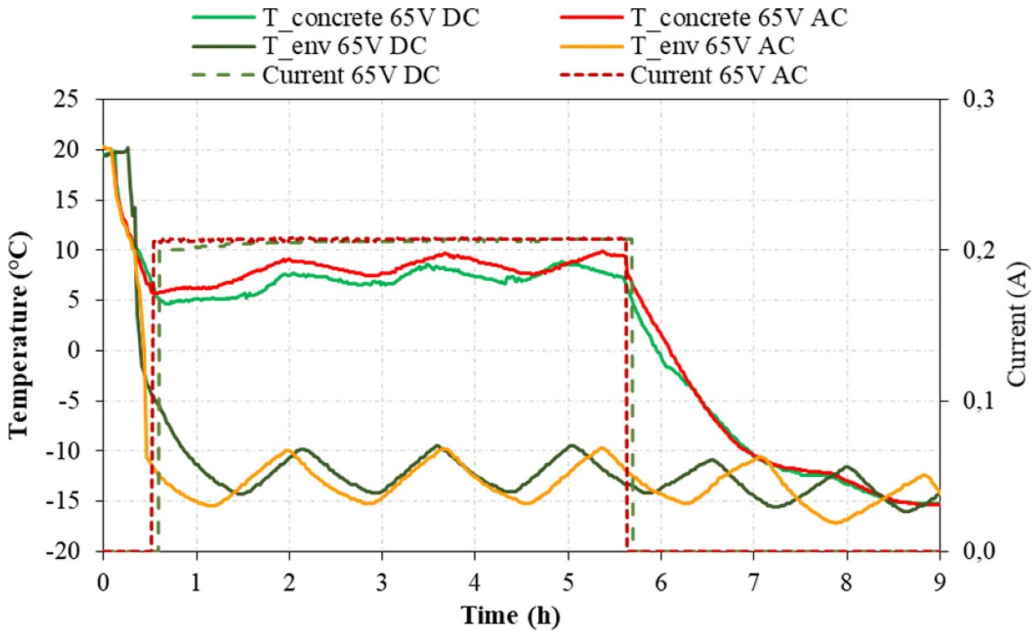

Figure 12. Environment (freezer) temperature (T_env), specimen's average temperature (T_concrete), both in °C, and the monitored current (dashed lines), in A, versus time, in h, for concrete 65 V fixed voltage AC and DC ice-preventing tests.

3.3. Study of de-icing and ice-prevention, in conductive concrete

Concerning de-icing tests, figure 11 shows the evolution of the temperature and the electrical current of a conductive concrete specimen. As it can be observed, a fixed voltage of 65 V (both AC and DC), was able to increase the temperature of the specimens above 0 °C in about 1 h, and above +5 °C in about 2.5 h. The maximum temperature registered was 9.2 °C with AC and 8.6 °C with DC. The average current was 0.202 A for AC and 0.206 A for DC and the average power, in W m^{-2}, was 196 and 200 for AC and DC tests, respectively. After approximately 5 h, the power sources were turned off. The same test was performed with different specimens with negligible behaviour differences.

Concerning ice-prevention tests, figure 12 shows the evolution of the temperature and the electrical current of a conductive concrete specimen. It is clear that no significant differences are observed between carrying out the experiment in AC or in DC test. Furthermore, preventing the formation of ice could be feasible by applying a 65 V voltage to the system.

Table 8. Summary of the electrical (resistivity, current type and fixed voltage applied), temperature (variation and absolute) and energy characteristics (average power, consumed energy and average energy consumption) of ice-prevention and de-icing tests.

	Resistivity (Ω°cm)	AC/DC	Voltage (V)	ΔT (°C)	T (°C)	Average power (W m^{-2})	Consumed energy (kW·h)	Average energy consumption (kW h m^{-2})
Ice-prevention	1062	DC	65	21.1	7	200	0.0668	1.00
	1055	AC	65	22.9	8.1	201	0.0673	1.00
De-icing	1058	DC	65	22	7.2	200	0.0671	1.00
	1079	AC	65	22.2	7	196	0.0658	0.98

As it can be observed, the results obtained were once more similar for both AC and DC tests. A fixed voltage of 65 V, both AC and DC, was able to maintain the temperature of the specimen above 0 °C. The maximum temperature registered was 10.0 °C with AC and 8.9 °C with DC. The average current was 0.207 A and 0.206 A for AC and DC tests, respectively, with an average power, in W m^{-2}, of 201 and 200 for AC and DC tests, respectively. These results are quite similar to the ones obtained in de-icing tests.

Table 8 summarizes the previous results for ice-preventing tests and de-icing tests, and includes the resistivity, the consumed energy and the average energy consumption or energy intensity per unit of area. All results are similar to the ones obtained in heating tests at the same conditions (see table 7), which indicates reliable system stability. As the energy consumption is low, this composite could turn into an environmentally friendly and cost-effective de-icing method.

The variation of temperature between the initial environment temperature and the final temperature of the specimens were similar in de-icing tests, ice-prevention tests and heating (at room temperature) tests, when applying the same voltage.

Considering a value of 0.15€ kW^{-1} h^{-1} and 5 h testing, the average cost would be 0.151 € m^{-2}, which is similar to the one calculated in heating tests (for the same fixed voltage, i.e. 65 V). The consumed energy is also similar.

4. Conclusions

(a) Heating function can be developed in conductive cement pastes with the hybrid addition of both CNT and GP (1% C100 + 5% ABG1010). Negligible differences in the behaviour were monitored when applying DC or AC.
(b) It is feasible to model the phenomenon in order to validate the mechanism of heating. An increment of +50 °C was obtained for both AC and DC, with fixed voltage of 40 V and electrical current around 640 mA.
(c) Heating, de-icing and ice-prevention functions can be developed in conductive concrete small slabs with the hybrid addition of both CNT and GP (specimens with 1%C100 + 5%ABG1010). This concrete showed low resistivity (1060 Ω cm).

Acknowledgments

The authors would like to acknowledge financial support received from European Union's Horizon 2020 Research and Innovation Programme under Grant Agreement No. 760940 and from the Generalitat Valenciana (Spain) (AICO/2019/050).

ORCID iDs

C Farcas https://orcid.org/0000-0003-4391-0082
O Galao https://orcid.org/0000-0003-0458-1845
R Navarro https://orcid.org/0000-0001-5565-0084
E Zornoza https://orcid.org/0000-0003-2302-5115
F J Baeza https://orcid.org/0000-0002-6837-3423
B Del Moral https://orcid.org/0000-0003-0906-3836
R Pla https://orcid.org/0000-0001-8040-4846
P Garcés https://orcid.org/0000-0002-4075-1365

References

[1] d'Alessandro A, Materazzi A L and Ubertini F 2020 *Nanotechnology in Cement-Based Construction* (Singapore: Jenny Stanford Publishing) (https://doi.org/10.1201/9780429328497)
[2] Galao O, Baeza F J, Zornoza E and Garcés P 2017 Carbon nanofiber cement sensors to detect strain and damage of concrete specimens under compression *Nanomaterials* **7** 413–27
[3] Baeza F J, Galao O, Zornoza E and Garcés P 2013 Multifunctional cement composites strain and damage sensors applied on reinforced concrete (RC) structural elements *Materials* **6** 841–55
[4] Ubertini F *et al* 2014 Novel nanocomposite technologies for dynamic monitoring of structures: a comparison between cement-based embeddable and soft elastomeric surface sensors *Smart Mater. Struct.* **23** 45023
[5] Camacho-Ballesta C, Zornoza E and Garcés P 2016 Performance of cement-based sensors with CNT for strain sensing *Adv. Cem. Res.* **28** 274–84
[6] Pérez A, Climent M A and Garcés P 2010 Electrochemical extraction of chlorides from reinforced concrete using a conductive cement paste as the anode *Corros. Sci.* **52** 1576–81
[7] Carmona J, Garcés P and Climent M A 2015 Efficiency of a conductive cement-based anodic system for the application of cathodic protection, cathodic prevention and electrochemical chloride extraction to control corrosion in reinforced concrete structures *Corros. Sci.* **96** 102–11

[8] del Moral B, Galao Ó, Antón C, Climent M A and Garcés P 2013 Usability of cement paste containing carbon nanofibres as an anode in electrochemical chloride extraction from concrete *Mater. Constr.* **63** 39–48
[9] Chung D D L 2001 Functional properties of cement-matrix composites *J. Mater. Sci.* **36** 1315–24
[10] Yehia S and Tuan C Y 1999 Conductive concrete overlay for bridge deck deicing *ACI Mater. J.* **96** 382–90
[11] Chung D D L 2004 Self-heating structural materials *Smart Mater. Struct.* **13** 562–5
[12] Norambuena-Contreras J, Quilodran J, Gonzalez-Torre I, Chavez M and Borinaga-Treviño R 2018 Electrical and thermal characterisation of cement-based mortars containing recycled metallic waste *J. Cleaner Prod.* **190** 737–51
[13] Gomis J, Galao O, Gomis V, Zornoza E and Garcés P 2015 Self-heating and deicing conductive cement. Experimental study and modeling *Constr. Build. Mater.* **75** 442–9
[14] Galao O, Bañón L, Baeza F J, Carmona J and Garcés P 2016 Highly conductive carbon fiber reinforced concrete for icing prevention and curing *Materials* **9** 281–95
[15] Sassani A *et al* 2018 Carbon fiber-based electrically conductive concrete for salt-free deicing of pavements *J. Cleaner Prod.* **203** 799–809
[16] Faneca G, Ikumi T, Torrents J M, Aguado A and Segura I 2020 Conductive concrete made from recycled carbon fibres for self-heating and de-icing applications in urban furniture *Mater. Constr.* **70** 223
[17] Galao O, Baeza F J, Zornoza E and Garcés P 2014 Self-heating function of carbon nanofiber cement pastes *Mater. Constr.* **64** e015
[18] Qin Z, Wang Y, Mao X and Xie X 2009 Development of graphite electrically conductive concrete and application in grounding engineering *New Build. Mater.* **11** 46–8
[19] Liebscher M, Tzounis L, Junger D, Dinh T T and Mechtcherine V 2020 Electrical Joule heating of cementitious nanocomposites filled with multi-walled carbon nanotubes: role of filler concentration, water content, and cement age *Smart Mater. Struct.* **29** 125019
[20] Dehghani A and Aslani F 2020 The effect of shape memory alloy, steel, and carbon fibres on fresh, mechanical, and electrical properties of self-compacting cementitious composites *Cem. Concr. Compos.* **112** 103659
[21] Xiang Z-D, Chen T, Li Z-M and Bian X-C 2009 Negative temperature coefficient of resistivity in lightweight conductive carbon nanotube/polymer composites *Macromol. Mater. Eng.* **294** 91–5
[22] Kim G M, Naeem F, Kim H K and Lee H K 2016 Heating and heat-dependent mechanical characteristics of CNT-embe-dded cementitious composites *Compos. Struct.* **136** 162–70
[23] Tuan C Y and Yehia S 2004 Evaluation of electrically conductive concrete containing carbon products for deicing *ACI Mater. J.* **101** 287–93
[24] del Moral B *et al* 2020 The effect of different oxygen surface functionalization of carbon nanotubes on the electrical resistivity and strain sensing function of cement pastes *Nanomaterials* **10** 1–15
[25] Wang S, Wen S and Chung D 2004 Resistance heating using electrically conductive cements *Adv. Cem. Res.* **16** 161–6
[26] Zhang K, Han B and Yu X 2011 Nickel particle based electrical resistance heating cementitious composites *Cold Reg. Sci. Technol.* **69** 64–9